Majorana Edge States for Z_2 Topological Orders of the Wen-plaquette Model and the Toric-code Model

Jing Yu,[1,2] Xing-Hai Zhang,[1] and Su-Peng Kou[1,*]

[1] *Department of Physics, Beijing Normal University, Beijing, 100875 P. R. China*
[2] *Department of Physics, Liaoning Shihua University, Fushun, 113001 P. R. China*

In this paper we study the symmetry protected Majorana edge states for the Z_2 topological order of the Wen-plaquette model and the toric-code model and calculate the dispersion of the Majorana edge states. For the system with translational symmetry, the Majorana edge states are gapless and have the nodal points at $k = 0$ and $k = \pi$. For the edge states of the toric-code model without translational symmetry, the edge modes become gapped.

I. INTRODUCTION

Topological properties of topologically ordered states can be partially characterized by their gapless edge states[1–4]. For example, the fractional quantum hall(FQH) states possess robust gapless edge modes as protected by the energy gap of the bulk, which can be derived from the Laughlin wave function[5]. On the other hand, people can obtain the bulk properties from the information of the edge states by bulk-boundary correspondence. For example, edge excitation of FQH states is chiral Luttinger liquid[1, 2] while that of non-Abelian FQH states[6] is more exotic and related to (1+1)-dimensional conformal field theories[3, 7].

Recently, several exactly solvable spin models are found with non-Abelian topological ordered state or Z_2 topological ordered state as the ground states, such as the toric-code model[8], the Wen-plaquette model[4, 10] on a square lattice and the Kitaev model on a honeycomb lattice[9]. In non-Abelian topological order of the Kitaev model on a honeycomb lattice the elementary excitation becomes non-Abelian anyon with nontrivial statistics. And the edge state is 1D gapless chiral Majorana modes. However, for a simpler example of a topological order - Z_2 topological order, gapless edge states have not been found while a gapped edge state may exist[11–14] instead. In the toric-code model, it is pointed out that there are two distinct types of boundaries (the smooth one and the rough one) with gapped edge states[11, 12]. We call them all zigzag boundary in this paper.

In this paper, instead of considering the zigzag boundaries that have gapped edge states, we study the Wen-plaquette model and the toric-code model with a new type of smooth boundary (which differs from the the smooth edge in Ref.[11, 12]) and use Majorana formulation to derive the effective theory of the gapless edge states. See the illustrations below. The gapless edge states are protected by translational symmetry along the boundary. When the translational symmetry is broken, the edge modes will have energy gap.

The paper is organized as follows. In Sec.II, we study the edge states of the Wen-plaquette model. In this section, we give the definition of the edge states by string operators and use the Majorana representation to describe Majorana edge states. In Sec.III we study the edge states of the toric-code model by similar approach. Finally, the conclusions are given in Sec.V.

II. THE EDGE STATES OF THE WEN-PLAQUETTE MODEL

A. The Wen-plaquette model

The Wen-plaquette model is defined on square lattice with the Hamiltonian

$$\hat{H} = -g \sum_i \hat{F}_i, \tag{1}$$

with

$$\hat{F}_i = \hat{\sigma}_i^x \hat{\sigma}_{i+\hat{e}_x}^y \hat{\sigma}_{i+\hat{e}_x+\hat{e}_y}^x \hat{\sigma}_{i+\hat{e}_y}^y \tag{2}$$

and $g > 0$. $\hat{\sigma}_i^x$, $\hat{\sigma}_i^y$ are Pauli matrices on site i.

The ground states of the Wen-plaquette model are known as Z_2 topological state[4, 10]. The ground state is denoted by $F_i \equiv +1$ at each plaquette. For this model, the elementary excitations are Z_2 vortex (m type excitation denoted by $F_i = -1$ at even sub-plaquette) and Z_2 charge (e type excitation denoted by $F_i = -1$ at odd sub-plaquette). In addition, there is a mutual-semion statistics between Z_2 vortex and Z_2 charge. A Z_2 vortex and a Z_2 charge annihilate with each other into a fermionic Z_2 link-excitation which is a pair of Z_2 vortex and Z_2 charge. The fermions have flat band - the energy spectrum is $E(\mathbf{k}) = 4g$, which implies that they cannot move at all.

The ground states of Z_2 topological state have topological degeneracy. Under the periodic boundary condition (on a torus), the ground states of the Wen-plaquette model have four-fold degeneracy on even-by-even ($e * e$) lattice, two-fold degeneracy on even-by-odd, odd-by-even and odd-by-odd lattices. For a system on a cylinder, the ground states have two-fold degeneracy. Physically, the topological degeneracy arises from the presence or the absence of π flux of fermions through the hole, as illustrated in Fig. 1.

*Corresponding author; Electronic address: spkou@bnu.edu.cn

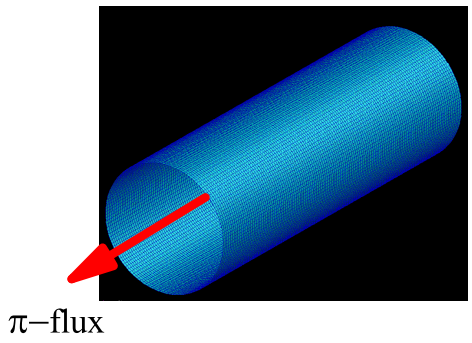

FIG. 1: The illustration of a system on a cylinder. The topological degeneracy arises from the presence or the absence of π flux of fermions through the hole.

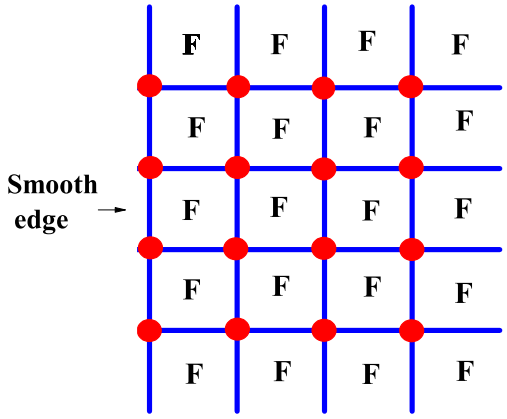

FIG. 2: The illustration of a smooth boundary of the Wen-plaquette model. The boundary has translational symmetry.

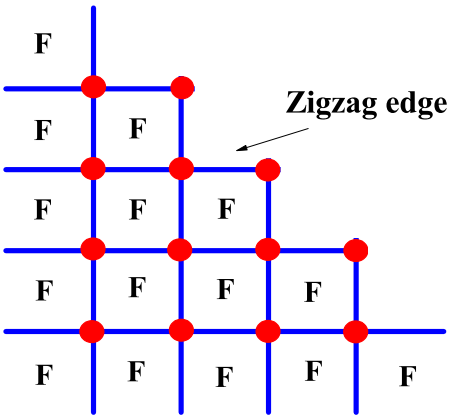

FIG. 3: The illustration of a zigzag boundary of the Wen-plaquette model. The boundary has no translational symmetry.

B. String representation of the edge states for the Wen-plaquette model

In Ref.[15], it is pointed out that for the Wen-plaquette model with smooth open boundary condition, there exist gapless edge states. Fig.2 shows the Wen-plaquette model with a smooth open boundary and Fig.3 shows the Wen-plaquette model with a zigzag open boundary. For a finite $L_x \times L_y$ lattice with a periodic boundary condition only along y-direction, there are two edges along y-direction. This model can be realized by setting $g = 0$ for one column of plaquettes and it remains exactly solvable. The ground states have $\sim 2^{L_y}$-fold degeneracy and can be viewed as gapless edge excitations on both boundaries described by Majorana fermion. These gapless edge states can be mapped to a Majorana fermion system with flat band exactly. Above argument comes from the exactly solvable model. But how the edge states change when there exist external fields? From the effective Z_2E type mutual U(1)×U(1) Chern-Simons(CS) theories of Z_2 topological order of the Wen-plaquette model, we have shown that there are right-moving and left-moving gapless edge excitations described by Majorana fermions, provided that the edge is in the x- or y-direction[15]. The presence of the translational symmetry in the x- or y-direction is crucial for the existence of the gapless edge excitations for the Z2E type mutual U(1)×U(1) CS theory and the lattice model. In addition, from the classification of the Z_2 topological order on a square lattice, we found that the emergent Majorana edge states of the Wen-plaquette model will always gapless at $k_x = 0, \pi$ (or $k_y = 0, \pi$) in momentum space[16, 17].

To describe the edge states of the ground states (the planar codes), we define the fermion string operators. In the bulk, the fermion string operators are $\hat{W}_f(C) = \prod_m \hat{\sigma}_{i_m}^{l_m}$[18], where C is a string connecting the middle of the nearby sites, and i_m are sites on the string. $l_m = z$ if the string does not turn at site i_m. $l_m = x$ or y if the string makes a turn at site i_m. $l_m = y$ if the turn forms a upper-right or lower-left corner. $l_m = x$ if the turn forms a lower-right or upper-left corner. Taking the open boundary condition into account, the loop C can be different. For system with open boundary condition, C is a string from one boundary to another. It is obvious that there are two kinds of strings, one has two ends at the same boundary (we call it C_s), the other terminates at different boundaries (we call it C_l). See Fig.4.

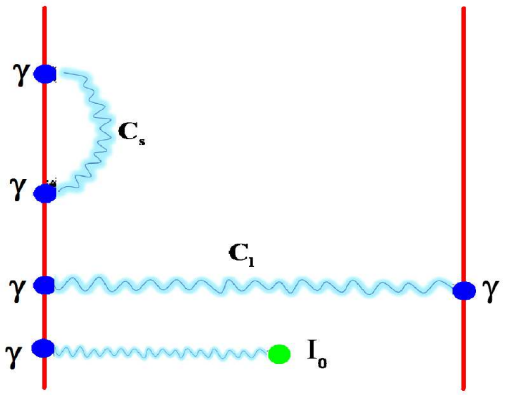

FIG. 4: The illustration of three fermion strings: the closed string C_s corresponds to the string with two ends at the same boundary; another closed string operator C_l corresponds to the string with two ends at the different boundaries; the third corresponds to the open fermion string with one end (the blue spot) on the boundary and the other (the green spot) in the bulk (site I_0 in the bulk). There exists Majorana fermion mode on each end of the open string.

Now we can create the edge states $|\text{edge}\rangle$ by performing a fermion string operation $\hat{W}_f(C_{s/l})$ connecting the boundaries on the ground state $|0\rangle$ as

$$|\text{edge}\rangle = \hat{W}_f(C_{s/l})\,|0\rangle\,.$$

Both the edge states $|\text{edge}\rangle$ and the ground states $|0\rangle$ can be denoted by $F_i \equiv +1$ at each plaquette and have the same ground state energy as

$$E_0 = \hat{H}_{\text{w}}\,|\text{edge}\rangle = H_{\text{w}}\,|0\rangle\,.$$

It is obvious that for the Wen-plaquette model, both types of fermion strings connecting the boundaries are condensed. These edge states have exact zero energy or flat band.

Let's explain why the edge states are really Majorana fermions. People know that for an open fermion string, there exists a Majorana fermion modes at each end. In Fig.4, we have shown an open fermion string, of which one end (the blue spot) is on the boundary, the other (the green spot) is in the bulk (site I_0 in the bulk). The end of fermion string in the bulk corresponds to a Majorana fermion mode. Since the fermion parity of system is conserved, there must exist another Majorana fermion mode at the boundary of the system which is another end of the fermion string (site i on the boundary). Thus each end of the fermion string connecting the boundaries corresponds to a Majorana fermion mode. On the other hand, each fermion string connecting the boundaries corresponds to a two-level state denoted by $\hat{W}_f(C_{s/l})\,|0\rangle = \pm\,|0\rangle$. Then we can say that each end of the fermion string connecting the boundaries is really a Majorana fermion mode.

There are two types of fermion string operators, $\hat{W}_f(C_s)$ denotes the string with two ends at the same boundary, $\hat{W}_f(C_l)$ denotes the string with two ends at the different boundaries.

When we add external field terms

$$\hat{H}_I = h^x \sum_i \hat{\sigma}_i^x + h^y \sum_i \hat{\sigma}_i^y + h^z \sum_i \hat{\sigma}_i^z, \qquad (3)$$

the degeneracy of the edge states will be removed and we will get the dispersive edge states. In the following parts we will calculate the dispersion of these edge states and point out that for the Wen-plaquette model with smooth boundary the gapless edge states are protected by the translational symmetry.

In addition, for this case, the edge states on a finite $L_x \times L_y$ lattice with a periodic boundary condition only along y-direction always have two-fold degeneracy. The two-fold degeneracy is characterized by the closed string operator along x-direction $\hat{W}_f(C_l) = \hat{\sigma}^z_{i+\hat{e}_x}\hat{\sigma}^z_{i+2\hat{e}_x}\cdots\hat{\sigma}^z_{i+L_x\hat{e}_x}$. For the case of $\hat{W}_f(C_l)\,|0\rangle = |0\rangle$, there is no π-flux inside the hole and the Majorana fermions on the edge have periodic boundary condition; for the case of $\hat{W}_f(C_l)\,|0\rangle = -\,|0\rangle$, there is a π-flux inside the hole and the Majorana fermions on the edge have anti-periodic boundary condition.

C. Majorana edge states for the Wen-plaquette model

In the following parts we will study the (symmetry protected) edge states by Majorana representation. Now we may use a Majorana mode γ_i to denote an end of the fermion string at boundary. For the boundary shown in Fig.2, the corresponding effective Hamiltonian of a single edge mode is given by

$$\hat{H}_{\text{edge}} = i\sum_{ij} J_{ij}\gamma_i\gamma_j \qquad (4)$$

where γ_i is the Majorana operators at edge position i, and obeys algebra relation $\{\gamma_i,\gamma_j\} = \delta_{ij}, \quad (\gamma_i)^\dagger = \gamma_i$.

1. *Quantum tunneling effect of Majorana modes*

Firstly, we select the Majorana edge states characterized by fermion string operator $\hat{W}_f(C_s) = \prod_m \hat{\sigma}^{l_m}_{i_m}$. A fermion string operator $\hat{W}_f(C_s)$ that connects the two points on boundary can be considered as quantum tunneling processes of virtual quasi-particles moving along the path. The quantum tunneling process of fermions is defined as : at first a single (bulk) fermion and an edge fermion are created together. Then this bulk fermion propagates and disappears at the boundary site j. And a string of $\hat{\sigma}_i^m$ is left on the tunneling path behind the virtual fermion, that is just a string operator $\hat{W}_f(C_s)$.

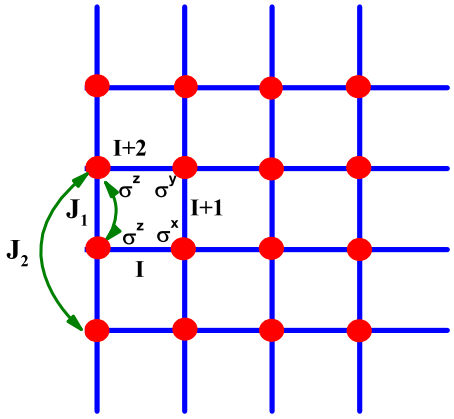

FIG. 5: The illustration of the relation between the hopping parameter J_1 in the effective model of the edge states and the quantum tunneling process. There is translational symmetry for the edge states along the boundary.

For simplicity, we use $|0\rangle$ and $|1\rangle$ to describe the two degenerate eigenstates of the string operator $\hat{W}_f(C_s)$, as

$$\hat{W}_f(C_s)\,|0\rangle = |0\rangle\,,\ \hat{W}_f(C_s)\,|1\rangle = -\,|1\rangle\,.$$

With the perturbation term $\hat{H}_I$, the quantum tunneling processes occur - the fermion propagates from one end of the string to the other. Thus we can use the quantum tunneling theory in Ref.[19, 20] to obtain the hopping parameters for the Majorana modes, J_{ij}. The nearest neighbor hopping parameter J_1 of the Majorana edge modes corresponds to the shortest fermion string with two ends at the same boundary, of which the fermion string operator is $\hat{W}_f(C_s) = \hat{\sigma}^z_i\hat{\sigma}^x_{i+\hat{e}_x}\hat{\sigma}^y_{i+\hat{e}_x+\hat{e}_y}\hat{\sigma}^z_{i+\hat{e}_y}$. See the illustration in Fig.5. And the next nearest neighbor hopping parameter J_2 corresponds to a fermion string with two ends at the same boundary, of which the fermion string operator is $\hat{W}_f(C_s) = \hat{\sigma}^z_i\hat{\sigma}^x_{i+\hat{e}_x}\hat{\sigma}^z_{i+\hat{e}_x+\hat{e}_y}\hat{\sigma}^y_{i+\hat{e}_x+2\hat{e}_y}\hat{\sigma}^z_{i+2\hat{e}_y}$.

Let's calculate J_1 by the higher order perturbation approach. From the higher order perturbation approach in Ref.[19, 20], we obtain the energy shifts of two eigenstates $|0\rangle$ and $|1\rangle$. We take the energy shifts of the quantum state $|1\rangle$ as an example which is

$$\delta E_1 = \langle 1|\,\hat{H}_I(\frac{1}{E_0-\hat{H}_0}\hat{H}_I)^{L_0-1}\,|1\rangle\,. \tag{5}$$

To calculate $(\frac{1}{E_0-\hat{H}_0}\hat{H}_I)\,|1\rangle$, we can choose site i as the starting point of the generation of an edge fermion mode and get

$$\begin{aligned}(\frac{1}{E_0-\hat{H}_0}\hat{H}_I)\,|1\rangle \to (\frac{h^z}{E_0-\hat{H}_0}\hat{\sigma}^z_i)\,|1\rangle \\ = (\frac{h^z}{E_0-\hat{H}_0})\,|\Psi_i\rangle\end{aligned} \tag{6}$$

where $|\Psi_i\rangle$ is the excited state of an edge fermion mode and a bulk fermion at link I (See Fig.5). From $\hat{H}_0\,|\Psi_i\rangle = (E_0+4g)\,|\Psi_i\rangle$, we have

$$(\frac{1}{E_0-\hat{H}_0}\hat{H}_I)\,|1\rangle = (\frac{h^z}{-4g})\,|\Psi_i\rangle\,.$$

Then the bulk fermion move from I-link to $I+1$-link by an $\hat{\sigma}^x_{i+\hat{e}_x}$ operation, then turn around to $I+2$-link by an $\hat{\sigma}^y_{i+\hat{e}_x+\hat{e}_y}$ operation. Finally, the bulk fermion disappears by performing the operation at $I+2$-link by $\hat{\sigma}^z_{i+\hat{e}_y}$ operation at site $i+1$.

Then we can get the energy shift of the state $\langle 1|$ as

$$\delta E_1 = \sum_{j=0}^{\infty}\langle 1|\,\hat{H}_I(\frac{1}{E_0-\hat{H}_0}\hat{H}_I)^j\,|1\rangle = \frac{h^x\,(h^z)^2\,h^y}{(-4g)^3}. \tag{7}$$

Using the same approach we can get the energy shift of the state $\langle 0|$ as

$$\delta E_0 = \sum_{j=0}^{\infty}\langle 0|\,\hat{H}_I(\frac{1}{E_0-\hat{H}_0}\hat{H}_I)^j\,|0\rangle = -\frac{h^x\,(h^z)^2\,h^y}{(-4g)^3}. \tag{8}$$

Finally an energy difference ε of the two quantum states is obtained as

$$\varepsilon = \delta E_1 - \delta E_0 = \frac{2h^x\,(h^z)^2\,h^y}{(-4g)^3} \tag{9}$$

which is the strength of the nearest neighbor hopping parameter J_1 of the Majorana edge modes,

$$\varepsilon = J_1 = \frac{2h^x\,(h^z)^2\,h^y}{(-4g)^3}.$$

Similarly we can derive the next nearest neighbor hopping parameter J_2 of the Majorana edge modes by using the same approach as

$$J_2 = \frac{2h^x\,(h^z)^3\,h^y}{(-4g)^4}. \tag{10}$$

2. *Symmetry protected Majorana edge states*

In this part, we use the Majorana representation to derive the dispersion of the Majorana edge states. By the following representation,

$$\gamma_i = \frac{1}{\sqrt{2}}\left(c_i + c_i^\dagger\right)\,,$$

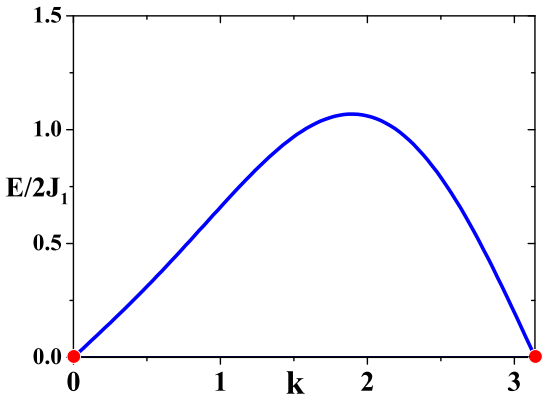

FIG. 6: The excited energies of a single edge mode of the Wen-plaquette model. The nodal points of Z_2 topological order are fixed at $k = 0$ and $k = \pi$ (the red spots). We have set $J_2 = -0.2J_1$.

we have

$$\begin{aligned}\hat{H}_{\text{edge}} &= i\sum_{\langle ij\rangle} J_1\gamma_i\gamma_j + i\sum_{\langle\langle ij\rangle\rangle} J_2\gamma_i\gamma_j + ... \\ &= \frac{iJ_1}{2}\sum_i (c_i + c_i^\dagger)(c_{i+1} + c_{i+1}^\dagger) \\ &+ \frac{iJ_2}{2}\sum_i (c_i + c_i^\dagger)(c_{i+2} + c_{i+2}^\dagger) + ... \\ &= \frac{iJ_1}{2}\sum_i [c_i^\dagger c_{i+1} - c_{i+1}^\dagger c_i + c_i^\dagger c_{i+1}^\dagger + c_i c_{i+1}] \\ &+ \frac{iJ_2}{2}\sum_i [c_i^\dagger c_{i+2} - c_{i+2}^\dagger c_i + c_i^\dagger c_{i+2}^\dagger + c_i c_{i+2}] \\ &+ ...\end{aligned} \tag{11}$$

In the momentum space we derive the energy spectrum of the edge states as

$$\begin{aligned}E_+ &\simeq 2(J_1\sin k + J_2\sin 2k), \\ E_- &= 0.\end{aligned} \tag{12}$$

Here the quantum states with zero energy are unphysical. Thus the excited energy of the edge states is given by

$$\Delta E = |E_+| = 2\left|J_1\sin k + J_2\sin 2k\right| .$$

We found that the nodal points of Z_2 topological order are fixed at $k = 0$ and $k = \pi$ on an edge which is protected by the Z_2 topological invariants and translational invariance. See Fig.6.

3. *Interference between the Majorana fermions on two boundaries*

In this part we study the interference between the Majorana fermions on two boundaries. Now the effective Hamiltonian of two coupling Majorana edge modes is given by

$$\begin{aligned}H_{\text{edge}} &\simeq i\sum_i J_t\gamma_{A,i}\gamma_{B,i} \\ &+ i\sum_i J_1\gamma_{A,i}\gamma_{A,i+1} + i\sum_i J_1\gamma_{B,i}\gamma_{B,i+1} \\ &+ i\sum_i J_2\gamma_{A,i}\gamma_{A,i+1} + i\sum_i J_2\gamma_{B,i}\gamma_{B,i+1}\end{aligned} \tag{13}$$

where A and B denote the indices of the two boundaries. J_t represents the coupling strength between two boundaries.

To derive J_t, we need to consider another type of string operators as $\hat{W}_f(C_l) = \hat{\sigma}^z_{i+\hat{e}_y}\hat{\sigma}^z_{i+2\hat{e}_y}\cdots\hat{\sigma}^z_{i+L_y\hat{e}_y}$. Such string operator is described by the quantum tunneling process of a link-fermion moving from one boundary to another along y-direction. The energy difference of the double states is

$$\varepsilon = -8g(\frac{h^z}{-4g})^{L_y} \to J_t. \tag{14}$$

Now L_y is not very big.

In addition, for a finite system we need to consider the quantum tunneling effect along x-direction which will remove the two-fold degeneracy of all quantum states including the edge modes. Because such quantum tunneling effect is characterized by the closed string operator $\hat{W}_f(C_l) = \hat{\sigma}^z_{i+\hat{e}_x}\hat{\sigma}^z_{i+2\hat{e}_x}\cdots\hat{\sigma}^z_{i+L_x\hat{e}_x}$ along x-direction, the energy splitting is about $-8g(\frac{h^z}{-4g})^{L_x}$. Here we consider the case with big L_x. Thus we can ignore this quantum tunneling effect.

For this case of $\hat{W}_f(C_l)\left|0\right\rangle = \left|0\right\rangle$, there is no π-flux inside the hole and the Majorana edges have periodic boundary condition. From $\gamma_{A,i} = \left(c_{A,i} + c_{A,i}^\dagger\right)/\sqrt{2}$ and

$\gamma_{B,i} = \left(c_{B,i} + c_{B,i}^\dagger\right)/\sqrt{2}$, we have

$$\begin{aligned}
\hat{H}_{\rm edge} \simeq\ & i\sum_i J_t \gamma_{A,i}\gamma_{B,i} \\
& + i\sum_i J_1 \gamma_{A,i}\gamma_{A,i+1} + i\sum_i J_1 \gamma_{B,i}\gamma_{B,i+1} \\
& + i\sum_i J_2 \gamma_{A,i}\gamma_{A,i+1} + i\sum_i J_2 \gamma_{B,i}\gamma_{B,i+1} \\
=\ & \frac{iJ_t}{2}\sum_i \left(c_{A,i} + c_{A,i}^\dagger\right)\left(c_{B,i} + c_{B,i}^\dagger\right) \\
& + \frac{iJ_1}{2}\sum_i \left(c_{A,i} + c_{A,i}^\dagger\right)\left(c_{A,i+1} + c_{A,i+1}^\dagger\right) \\
& + \frac{iJ_1}{2}\sum_i \left(c_{B,i} + c_{B,i}^\dagger\right)\left(c_{B,i+1} + c_{B,i+1}^\dagger\right) \\
& + \frac{iJ_2}{2}\sum_i \left(c_{A,i} + c_{A,i}^\dagger\right)\left(c_{A,i+2} + c_{A,i+2}^\dagger\right) \\
& + \frac{iJ_2}{2}\sum_i \left(c_{B,i} + c_{B,i}^\dagger\right)\left(c_{B,i+2} + c_{B,i+2}^\dagger\right). \quad (15)
\end{aligned}$$

In the momentum space we have

$$H_{\rm edge} = \sum_{k>0} (c_{A,k}, c_{A,-k}^\dagger, c_{B,k}, c_{B,-k}^\dagger)\epsilon(k) \begin{pmatrix} c_{A,k}^\dagger \\ c_{A,-k} \\ c_{B,k}^\dagger \\ c_{B,-k} \end{pmatrix} \quad (16)$$

where

$$\epsilon(k) = \begin{pmatrix} \varepsilon_k & \varepsilon_k & iJ_t/2 & iJ_t/2 \\ \varepsilon_k & \varepsilon_k & iJ_t/2 & iJ_t/2 \\ -iJ_t/2 & -iJ_t/2 & \varepsilon_k & \varepsilon_k \\ -iJ_t/2 & -iJ_t/2 & \varepsilon_k & \varepsilon_k \end{pmatrix} \quad (17)$$

and $\varepsilon_k = J_1 \sin k + J_2 \sin 2k$. Now we have the eigenvalues as

$$E = 0, 0, 2\left(J_1 \sin k + J_2 \sin 2k\right) \pm J_t\,. \quad (18)$$

In particular, for periodic boundary condition. The momentum is

$$k = \frac{2\pi n}{M},\ n = 1, 2..., M$$

where M is an integer number.

On the other hand, for the case of $W(C_l)\left|0\right\rangle = -\left|0\right\rangle$, there is a π-flux inside the hole and the Majorana edges have anti-periodic boundary condition. We have similar energy levels. However due to the anti-periodic boundary condition, the momentum is

$$k = \frac{2\pi n - \pi}{M},\ n = 1, 2..., M$$

where M is an integer number. The two cases are always degenerate for an infinite system.

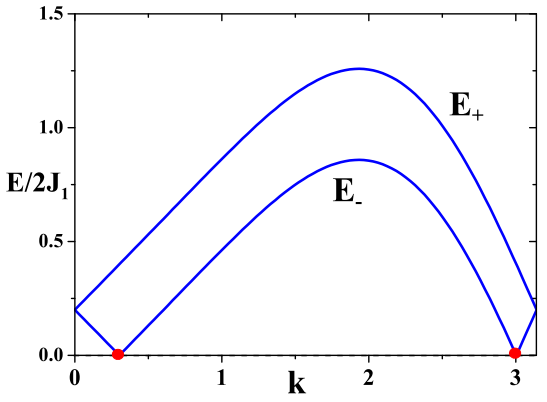

FIG. 7: The excited energies of two edge modes of the Wen-plaquette model with interference effect. The nodal points of Z_2 topological order shift away from $k = 0$ and $k = \pi$ (the red spots). We have set $J_2 = -0.2J_1$, $J_t = 0.2J_1$.

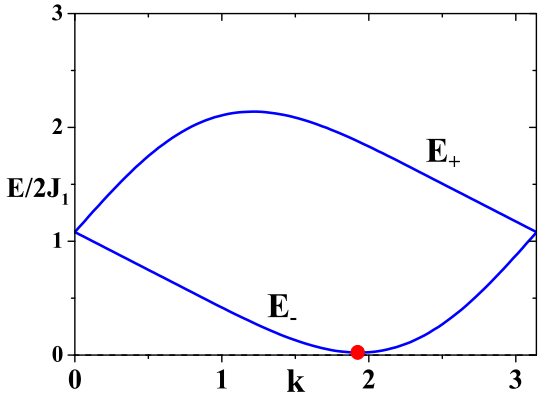

FIG. 8: The excited energies of two edge modes of the Wen-plaquette model with interference effect. There exists a gapless point with quadratic dispersion (the red spot). We have set $J_2 = -0.2J_1$, $J_t = 1.08J_1$.

Because the quantum states with zero energy are unphysical, the excited energies are

$$\begin{aligned} E_+ &= \left|2\left(J_1 \sin k + J_2 \sin 2k\right) + J_t\right|, \\ E_- &= \left|2\left(J_1 \sin k + J_2 \sin 2k\right) - J_t\right|. \end{aligned} \quad (19)$$

We found that the nodal points of Z_2 order are not fixed at $k = 0/\pi$ on an edge due to the interference effect between the Majorana fermions on two boundaries. See Fig.7. For $J_t > 1.08J_1$, the edge states become full gapped by mixing the edge states on different boundaries. See Fig.9.

In particular, for a special case $\hat{H}_I = h^z \sum_i \hat{\sigma}_i^z$, the bulk fermion can only move straightforwardly but cannot turn a corner. Now we have $J_1 = J_2 = 0$. Then

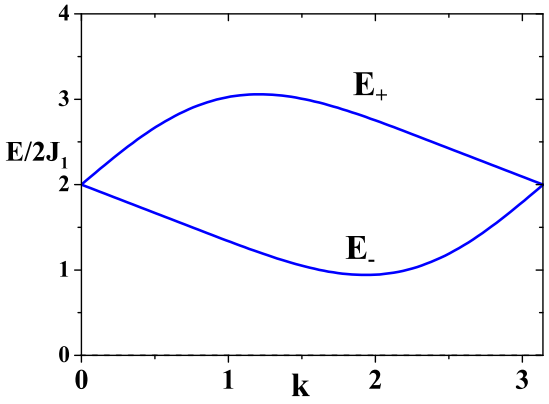

FIG. 9: The excited energies of two edge modes of the Wen-plaquette model with interference effect. The edge states are full gapped. We have set $J_2 = -0.2J_1$, $J_t = 2J_1$.

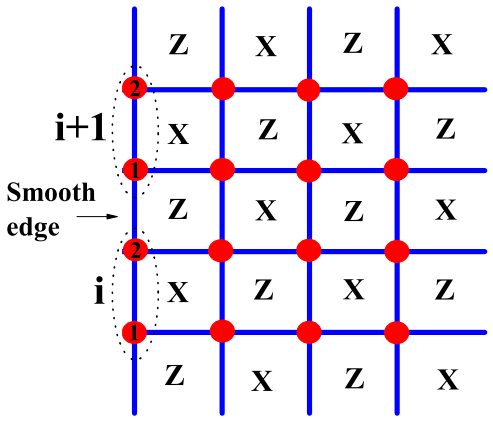

FIG. 10: The illustration of a smooth boundary of the toric-code model. The boundary has translational symmetry for the case of $A = B$. When there is no translational symmetry for the case of $A \neq B$, the unit-cell along the edge has two sites. Here we denote the unit-cells by i and $i+1$.

the effective Hamiltonian of two coupling Majorana edge modes becomes

$$\hat{H}_{\rm edge} = iJ_t \sum_i \gamma_{A,i}\gamma_{B,j}. \tag{20}$$

By the following representation of Majorana modes,

$$\gamma_{A,i} = \left(c_i + c_i^\dagger\right)/\sqrt{2}, \qquad \gamma_{B,i} = \left(c_i - c_i^\dagger\right)/(\sqrt{2}i),$$

we have

$$\begin{aligned}\hat{H}_{\rm edge} &= iJ_t \sum_i (c_i + c_i^\dagger)(-i)(c_i - c_i^\dagger) \\ &= J_t \sum_i c_i^\dagger c_i.\end{aligned}$$

This is a complex fermion system with two energy levels.

III. THE EDGE STATES OF THE TORIC-CODE MODEL

The toric-code model is described by the Hamiltonian [8]

$$\begin{aligned}\hat{H}_{\rm tc} = -A \sum_{i\in{\rm even}} \hat{Z}_i - B \sum_{i\in{\rm odd}} \hat{X}_i + \\ h^x \sum_i \hat{\sigma}_i^x + h^y \sum_i \hat{\sigma}_i^y + h^z \sum_i \hat{\sigma}_i^z.\end{aligned} \tag{21}$$

where

$$\hat{Z}_i = \hat{\sigma}_i^z \hat{\sigma}_{i+\hat{e}_x}^z \hat{\sigma}_{i+\hat{e}_x+\hat{e}_y}^z \hat{\sigma}_{i+\hat{e}_y}^z, \ \hat{X}_i = \hat{\sigma}_i^x \hat{\sigma}_{i+\hat{e}_x}^x \hat{\sigma}_{i+\hat{e}_x+\hat{e}_y}^x \hat{\sigma}_{i+\hat{e}_y}^x.$$

$\hat{\sigma}_i^{x,y,z}$ are Pauli matrices on sites, i. In this paper we only consider the case of $A > 0$, $B > 0$. The ground state of the toric-code model is also Z_2 topological state which is similar to that of the Wen-plaquette model. For the toric-code model, if we choose $A > 0$, $B > 0$, the ground state of it is denoted by $Z_i \equiv +1$ and $X_i \equiv +1$ at each plaquette.

A. String representation of the edge states for the toric-code model

To describe the edge states of the ground states (the planar codes), we also define the fermion string operators. In the bulk, the fermion string operators are also $\hat{W}_f(C) = \prod_m \hat{\sigma}_{i_m}^{l_m}$, where C is a string, and i_m are sites on the string. $l_m = y$ if the string does not turn at site i_m. $l_m = x$ or z if the string makes a turn at site i_m. $l_m = x$, if the string turns around the X-plaquette; $l_m = z$, if the string turns around the Z-plaquette. For system with open boundary condition, C is a string from one boundary to another. It is obvious that the two types of string operators correspond to the string with two ends at the same boundary (we call it C_s) and that with two ends at different boundaries (we call it C_l), respectively. See Fig.5. Similarly we can create the edge states $|{\rm edge}\rangle$ by doing a fermion string operation $\hat{W}_f(C_{s/l})$ connecting the boundaries on the ground state $|0\rangle$ as

$$|{\rm edge}\rangle = \hat{W}_f(C_{s/l})\,|0\rangle\,.$$

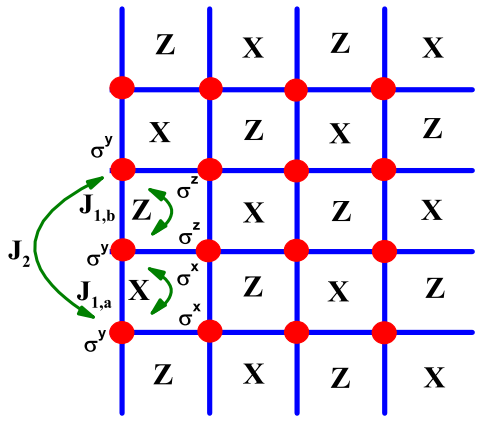

FIG. 11: The illustration of the relation between hopping parameters $J_{1,a}$, $J_{1,b}$ in the effective model of the edge states for the toric-code model and quantum tunneling processes.

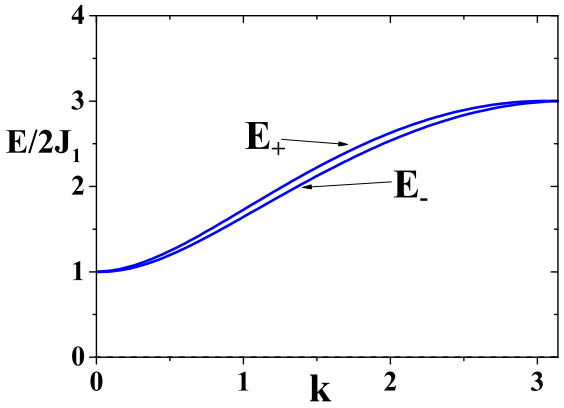

FIG. 12: The excited energies of a single edge mode of the toric-code model. The edge states are full gapped without translational symmetry. We have set $J_2 = -0.0125 J_{1,a}$ and $J_{1,b} = 0.5 J_{1,a}$. The spectrum splitting comes from a small next nearest neighbor hopping.

B. Majorana edge states for the toric-code model

Now we may use a Majorana mode γ_i to denote an end of the fermion string at boundary for the toric-code model. For the boundary shown in Fig.10, the boundary has translational symmetry for the case of $A = B$. When there is no translational symmetry for the case of $A \neq B$, the unit-cell along the edge has two sites. Here we denote the unit-cells by i and $i+1$. Now we have two-sublattice in a unit-cell and denote them by 1 and 2. The corresponding effective Hamiltonian of a single edge mode is given by

$$\hat{H}_{\rm edge} = iJ_{1,a}\sum_i \gamma_{1,i}\gamma_{2,i} + iJ_{1,b}\sum_i \gamma_{2,i}\gamma_{1,i+1} + iJ_2\sum_i \gamma_{1,i}\gamma_{1,i+1} + iJ_2\sum_i \gamma_{2,i}\gamma_{2,i+1}... \quad (22)$$

The nearest neighbor hopping parameters $J_{1,a}$ and $J_{1,b}$ of the Majorana edge modes correspond to the fermion string operators $\hat{W}_f(C_s) = \hat{\sigma}^y_i \hat{\sigma}^x_{i+\hat{e}_x} \hat{\sigma}^x_{i+\hat{e}_x+\hat{e}_y} \hat{\sigma}^y_{i+\hat{e}_y}$ and $\hat{W}_f(C_s) = \hat{\sigma}^y_i \hat{\sigma}^z_{i+\hat{e}_x} \hat{\sigma}^z_{i+\hat{e}_x+\hat{e}_y} \hat{\sigma}^y_{i+\hat{e}_y}$, respectively. See the illustration in Fig.11. And the next nearest neighbor hopping parameter J_2 corresponds the fermion string operator $\hat{W}_f(C_s) = \hat{\sigma}^y_i \hat{\sigma}^x_{i+\hat{e}_x} \hat{\sigma}^y_{i+\hat{e}_x+\hat{e}_y} \hat{\sigma}^z_{i+\hat{e}_x+2\hat{e}_y} \hat{\sigma}^y_{i+2\hat{e}_y}$. Similarly we can derive the nearest neighbor hopping parameter J_1 and the next nearest neighbor hopping parameter J_2 of the Majorana edge modes by using the same approach in above section as

$$J_{1,a} = \frac{2h^x (h^y)^2 h^x}{(-2A-2B)^3}, \; J_{1,b} = \frac{2h^z (h^y)^2 h^z}{(-2A-2B)^3}$$
$$J_2 = \frac{2h^x (h^y)^3 h^z}{(-2A-2B)^4}. \quad (23)$$

See Fig.11.

By defining $\gamma_{1,i} = (\psi_{1,i} + \psi^\dagger_{1,i})/\sqrt{2}$, $\gamma_{2,i} = (\psi_{2,i} - \psi^\dagger_{2,i})/(\sqrt{2}i)$, we have

$$H_{edge} = \frac{1}{2}\begin{pmatrix} \psi_{A,k} & \psi^\dagger_{A,-k} & \psi_{B,k} & \psi^\dagger_{B,-k} \end{pmatrix} \begin{pmatrix} 2J_2\sin k & 2J_2\sin k & -J_{1,a}+J_{1,b}e^{ik} & J_{1,a}-J_{1,b}e^{ik} \\ 2J_2\sin k & 2J_2\sin k & -J_{1,a}+J_{1,b}e^{ik} & J_{1,a}-J_{1,b}e^{ik} \\ -J_{1,a}+J_{1,b}e^{-ik} & -J_{1,a}+J_{1,b}e^{-ik} & 2J_2\sin k & -2J_2\sin k \\ J_{1,a}-J_{1,b}e^{-ik} & J_{1,a}-J_{1,b}e^{-ik} & -2J_2\sin k & 2J_2\sin k \end{pmatrix} \begin{pmatrix} \psi^\dagger_{A,k} \\ \psi_{A,-k} \\ \psi^\dagger_{B,k} \\ \psi_{B,-k} \end{pmatrix}.$$

The excited energies of the edge states are

$$E_+ = \left|2J_2\sin k + \sqrt{J^2_{1,a}+J^2_{1,b}-2J_{1,a}J_{1,b}\cos k}\right|,$$
$$E_- = \left|2J_2\sin k - \sqrt{J^2_{1,a}+J^2_{1,b}-2J_{1,a}J_{1,b}\cos k}\right|.$$

If $J_{1,a} = J_{1,b}$ (or $A = B$), the system has translational symmetry and the edge modes becomes gapless. In gen-

eral, due to $J_2 << J_{1,a}, J_{1,b}$, we have the full gapped edge modes. In Fig.12, we set $J_2 = 0.0125 J_{1,a}$ and $J_{1,b} = 0.5 J_{1,a}$.

IV. CONCLUSION

In this paper we study the symmetry protected Majorana edge states for the Z_2 topological order of the Wen-plaquette model and those of the toric-code model and calculate the dispersion of the Majorana edge states. We found that for the Wen-plaquette model the nodal points are fixed at $k = 0$ and $k = \pi$ on an edge which is protected by the Z_2 topological invariants and translational invariance. Due to the interference effect between the Majorana fermions on two boundaries, the nodal points of the Wen-plaquette model are not fixed at $k = 0/\pi$. For strong interference case, the edge states become full gapped. While, for the toric-code model with $A \neq B$, there is no translational symmetry along the edges. Then the edge modes becomes gapped. If we recover the translational symmetry by setting $A = B$, the edge states of the toric-code model have same properties to those of the Wen-plaquette model.

Acknowledgments

This work is supported by NFSC Grant No. 11174035, National Basic Research Program of China (973 Program) under the grant No. 2011CB921803, 2012CB921704.

[1] X.-G. Wen, Phys. Rev. **B 41**, 12838 (1990).
[2] X.-G. Wen, Phys. Rev. **B 43**, 11025 (1991).
[3] X. G. Wen, Int. J. Mod. Phys. **B 6**, 1711 (1992).
[4] X.-G. Wen, *Quantum Field Theory of Many-Body Systems*, (Oxford Univ. Press, Oxford, 2004).
[5] R. B. Laughlin, Phys. Rev. Lett. **50**, 1395 (1983).
[6] G. Moore and N. Read, Nucl. Phys. **B 360**, 362 (1991).
[7] X.-G. Wen, Y. S. Wu, Y. Hatsugai, Nucl. Phys. B422, 476 (1994)
[8] A. Kitaev, Ann. Phys. **303**, 2(2003).
[9] A. Kitaev, Ann. Phys. **321**, 2(2006).
[10] X.-G. Wen, Phys. Rev. Lett. **90** (2), 016803 (2003).
[11] S. B. Bravyi, A. Yu. Kitaev, arXiv:9811052.
[12] A. Kitaev, Liang Kong, arXiv:1104.5047.
[13] S. Beigi, P. Shor, D. Whalen, arXiv:1006.5479.
[14] X Chen, Z. X. Liu, X-G Wen, Phys. Rev. **B 84**, 235141 (2011).
[15] S. P. Kou, M. Levin, and X.-G. Wen, Phys. Rev. **B 78**, 155134 (2008).
[16] S. P. Kou and X.-G. Wen, Phys. Rev. **B 80**, 224406 (2009).
[17] S. P. Kou and X.-G. Wen, Phys. Rev. **B 82**1445012010.
[18] X.-G. Wen, Phys. Rev. **D 68**, 065003 (2003).
[19] S. P. Kou, Phys. Rev. Lett. **102**, 120402 (2009), S. P. Kou, Phys. Rev. **A**. **80**, 052317 2009.
[20] J. Yu and S. P. Kou, Phys. Rev. **B 80**, 075107 (2009).